



μ - Λ relationships for convective and stratiform rainfall in the Netherlands

Christos Gatidis¹, Marc Schleiss¹, and Christine Unal¹

¹Department of Geoscience and Remote Sensing, Delft University of Technology, Delft, The Netherlands

Correspondence: Christos Gatidis (C.Gatidis@tudelft.nl)

Abstract. In this study, we take a closer look at the important issue of μ - Λ relationships in raindrop size distributions (DSD) by conducting a systematic analysis of twenty months of rainfall data in the Netherlands. A new power-law model for representing μ - Λ relationships based on double normalization framework is proposed and used to derive separate μ - Λ relationships for stratiform and convective rain events. The sensitivity of the obtained relationships to measurement uncertainty is studied by applying two different quality control filters based on the mass-weighted mean drop diameter (D_m) and liquid water content (LWC). Our results show that there are significant differences in μ - Λ relationships between convective and stratiform rainfall types. However, the retrieved relationships appear to be quite robust to measurement noise and there is a good agreement with other reference relations for similar climatological conditions.



1 Introduction

10 The μ - Λ relationship in rainfall micro-physics refers to a deterministic function linking the shape (μ) and scale (Λ) parameters of a gamma raindrop size distribution (DSD) model (Zhang et al. (2001)). Such relationships are important for understanding the microstructure and dynamics of precipitation and are essential for retrieving DSDs from polarimetric radar measurements.

The primary use of μ - Λ relationships in radar remote sensing is to reduce the number of model parameters (from three to two) in DSD retrieval algorithms. However, DSD retrieval remains challenging and subject to various sources of uncertainty, including the accuracy of the remote sensing observations, the limitations of the DSD retrieval algorithms and the choice of the μ - Λ relationship.

Numerous μ - Λ relationships have been proposed in the literature, with second-order polynomial functions being the most popular. The first relationships were proposed by Zhang et al. (2001, 2003) using DSD data collected in Florida, USA. Since then, several other relationships have been proposed for different datasets and rainfall climatologies. For example, van Leth et al. (2020) derived a relationship for the Netherlands using nine months of disdrometer data in Wageningen. Their relationship differs from those reported by Zhang et al. (2001, 2003) which is reasonable given that stratiform rain dominates in the Netherlands and convective and stratiform precipitation have different DSDs. Notably, the drop sizes in convective rain tend to be larger and more variable, which results in a broader DSD with smaller μ and Λ values. Conversely, raindrops in stratiform rain are typically smaller and more uniform in size, corresponding to larger μ values for a given Λ . Vivekanandan et al. (2004) pointed out that correlation between μ and Λ exists but may vary across different types of rain, highlighting the need for further understanding of μ - Λ variability. Despite the fact that the μ - Λ relationship changes depending on rain-type, Chu and Su (2008) has shown that μ - Λ relations exhibit similar behaviour for small μ values, which usually correspond to heavier rainfall events, while the relations start to deviate as μ and Λ increase, indicating light to moderate rain events.

At the microphysics scale, Bringi et al. (2003) showed that a linear relationship with a negative slope exists between the generalized intercept parameter (N_w) in logarithmic scale and the mass-weighted mean diameter (D_m) for stratiform rainfall. For convective rain, two clusters of data emerge, with one cluster consisting of maritime-like convective points and the other of continental-like points. The latter is characterized by larger raindrop sizes and lower concentration, whereas the former exhibits the opposite trend, with a higher concentration of smaller-sized drops.

Similarly, other studies have examined discrepancies in μ - Λ relationships based on either regional (Chen et al. (2016)) or seasonal criteria (Seela et al. (2018)), showing that both factors are influenced by the prevailing climatic conditions and the dominant rain type. Besides the rain type and climatology, other factors that could potentially affect μ - Λ relation have also been partially investigated, such as sampling errors (Zhang et al. (2003)), temporal sampling resolution, and the adequacy of the gamma model itself (Gatidis et al. (2022)). Zhang et al. (2003) discussed how sampling errors or deviations from the gamma distribution could result in a correlation between μ and Λ . Using DSD observations of moderate-intensity, stratiform rain events in the Netherlands, Gatidis et al. (2022) found that the μ - Λ relationship remained robust regardless of the sampling resolution and the validity of the gamma model.



In this paper, we take a closer look at μ - Λ relationships in the Netherlands, highlighting the differences between convective and stratiform rain.

2 Data

45 The DSD data used in this study were collected by two co-located Parsivel² (Particle Size and Velocity) optical disdrometers at the Cabauw Experimental Site for Atmospheric Research (CESAR) observatory between Jan 1st 2021 and Aug 31st 2022. The sampling resolution was 1 minute. The measurement principle and characteristics of the Parsivel² have already been extensively described in previous studies Löffler-Mang and Joss (2000); Thurai et al. (2011); Tokay et al. (2014) and will not be repeated here.

50 In addition to the disdrometer data, the following resources were used for visualisation purposes and qualitative precipitation classification:

- Radar data collected by CLARA (CLOUD Atmospheric RADar), a dual-frequency (35-94 GHz) polarimetric scanning cloud radar in Cabauw.
- Vertical profiles of reflectivity from a micro rain radar (MRR) at Cabauw (<https://dataplatfom.knmi.nl/dataset/ruisdael-mrr-cabauw-2>).
- Convective available potential energy from ERA5, ECMWF reanalysis data, (<https://doi.org/10.24381/cds.adbb2d47>).
- Lightning activity (strikes) from the ZEUS long-range cloud-to-ground lightning detection system (<https://www.meteo.gr/talos/en/>).

3 Methodology

60 The methodology can be summarized as follows. Firstly, rain events are classified into two types: convective and stratiform. The data from the two co-located disdrometers are then used to fit a gamma model for each 1-min time interval and derive the corresponding shape (μ) and scale (Λ) parameters. The data from the two disdrometers are cross-checked and any time steps for which the two sensors disagree with each other are removed. The remaining data are used to fit the overall μ - Λ relation, as well as the relations for convective and stratiform rainfall types. Finally, the results are compared with those available in the
65 literature to ensure consistency and validity.



3.1 DSD model / Parameter fitting

The DSD $N(D)$ ($\text{mm}^{-1} \text{m}^{-3}$) is modeled using a normalized gamma distribution with shape parameter μ (-), slope Λ (mm^{-1}) and intercept N_w ($\text{mm}^{-1} \text{m}^{-3}$) as in (Bringi et al. (2003); Testud et al. (2001)):

$$N(D) = N_w f(\mu) \left(\frac{D}{D_m} \right)^\mu e^{-(4+\mu) \frac{D}{D_m}} \quad (1)$$

$$70 \quad f(\mu) = \frac{6}{4^4} \frac{(\mu+4)^{(\mu+4)}}{\Gamma(\mu+4)}, \quad (2)$$

$$N_w = \frac{4^4}{\pi \rho_w} \left(\frac{\text{LWC}}{D_m^4} \right), \quad (3)$$

$$D_m = \frac{4 + \mu}{\Lambda}. \quad (4)$$

In the equations above, D_m (mm) is the mass-weighted mean diameter, LWC (g m^{-3}) the liquid water content and ρ_w (10^{-3}g mm^{-3}) the density of liquid water. This model has been extensively used and assessed in the literature and will not be
75 discussed any further here (Gatidis et al. (2020); Thurai et al. (2019)). To estimate the three unknown parameters μ , Λ and N_w from empirical DSD spectra, the method of moments (Gatidis et al. (2022, 2020); Thurai et al. (2014)) is used, with μ values ranging between -3 and 15, as described in Thurai et al. (2014).

3.2 μ - Λ relationship

Numerous empirical μ - Λ relationships have been proposed and discussed in the literature (Zhang et al. (2003); van Leth et al.
80 (2020); Gatidis et al. (2022)). The most common is the second-order polynomial model proposed by Zhang et al. (2001):

$$\mu = -0.016\Lambda^2 + 1.213\Lambda - 1.957. \quad (5)$$

While polynomial relationships are a practical way to represent empirical μ - Λ relationships, they lack theoretical justification, and their coefficients do not have clear physical interpretations. Thus, we propose an alternative model that offers better justification and interpretation. Our model is:

$$85 \quad \Lambda = \alpha(\mu+3)^\beta (\mu+4)^{1-\beta}, \quad (6)$$

where α (mm^{-1}) and β (-) are two model coefficients inferred using a non-linear least squares fit on pairs of (μ, Λ) values.



Justification:

The $\mu - \Lambda$ relationship in Eq. (6) can be derived from the double-moment normalization framework by Lee et al. (2004). In this framework, the DSD is expressed as $N(D) = N_c h(\frac{D}{D_c})$ where D_c (mm) is a characteristic drop diameter that depends on two references moments, N_c ($\text{mm}^{-1} \text{m}^{-3}$) is a drop number concentration parameter and h a template function for describing the shape of the normalized DSD. The two reference moments M_i and M_j used for the normalization depend on the application. In all generality:

$$D_c = \left(\frac{M_j}{M_i} \right)^{\frac{1}{j-i}}, \quad (7)$$

$$N_c = M_i^{(j+1)(j-i)} M_j^{(i+1)(i-j)}. \quad (8)$$

To simplify, we consider the special case in which $j = i + 1$ and $D_c = M_j/M_{j-1}$. For example, when $j=4$ and $i=3$, we get $D_c = M_4/M_3 = D_m$. If in addition we assume that the DSD is gamma, then we get the model for $N(D)$ as in Eq. (1).

One key property of the double-moment normalization framework is that any moment M_n of the DSD can be expressed as a power law of the characteristic drop size D_c :

$$M_n = \int_{D=0}^{\infty} D^n N(D) dD = N_c \xi_n D_c^{n+1}, \quad (9)$$

where

$$\xi_n = \int_0^{\infty} x^n h(x) dx. \quad (10)$$

However, since the DSD variability might not be fully captured by two reference moments, we will assume that:

$$M_n = N_c a_n D_c^{b_n}, \quad (11)$$

where a_n and b_n are two empirical coefficients which can be slightly different from their theoretical expressions in Eq. (9).

Assuming Eq. (11) holds, we must have:

$$\frac{M_n}{M_{n-1}} = \frac{a_n}{a_{n-1}} D_c^{b_n - b_{n-1}}. \quad (12)$$

If the DSD is gamma and D_c is the ratio of two successive reference moments $i = j - 1$, then D_c is given by:

$$D_c = \frac{M_j}{M_{j-1}} = \frac{\mu + j}{\Lambda}. \quad (13)$$



Combining Eq. (12) and Eq. (13) yields:

$$110 \quad \frac{M_n}{M_{n-1}} = \frac{a_n}{a_{n-1}} \left(\frac{\mu + j}{\Lambda} \right)^{b_n - b_{n-1}}. \quad (14)$$

For a gamma DSD, the left hand side is: $\frac{\mu+n}{\Lambda}$. Therefore,

$$\frac{\mu + n}{\Lambda} = \frac{a_n}{a_{n-1}} \left(\frac{\mu + j}{\Lambda} \right)^{b_n - b_{n-1}}, \quad (15)$$

which can be rewritten as:

$$\Lambda = \alpha_n (\mu + n)^{\beta_n} (\mu + j)^{1 - \beta_n}, \quad (16)$$

115 where $\beta_n = (b_{n-1} - b_n + 1)^{-1}$ and $\alpha_n = \left(\frac{a_{n-1}}{a_n} \right)^{\beta_n}$. This leads to a general $\mu - \Lambda$ relationship of the form:

$$\Lambda = \alpha (\mu + n)^\beta (\mu + j)^{1 - \beta}, \quad (17)$$

where α and β depend on the two chosen pairs of consecutive reference moments (M_{j-1}, M_j) and (M_{n-1}, M_n). In particular, if $n=3$ and $j=4$, then we get $D_c = D_m$ and Eq. (6), which is the equation we will use in this study. Note that the choice $n=j$ is impossible because it just leads to a self-consistency constraint $D_c = \frac{\mu+4}{\Lambda}$. In other words, for any characteristic drop size D_c ,
 120 two additional moments are needed to estimate the scaling law linking M_n to D_c .

Eq. (17) is interesting because it shows that within the framework of double-moment normalization, the relationship between μ and Λ depends on the chosen reference moments used to fit and/or model the DSD. This is a finding that had been previously reported by other studies, such as Seifert (2005), but has not been fully explained until now.

3.3 Stratiform/Convective classification

125 Several methods have been proposed to classify rainfall into stratiform and convective regimes using disdrometers, weather radar, or a combination of both (Ulbrich and Atlas (2007); Tokay and Short (1996)). One popular method referred to as BR03 Brangi et al. (2003) uses the standard deviation of the rain rate over a 10-minute moving time window. If the standard deviation exceeds 1.5 mm h^{-1} , the period is classified as convective; otherwise, it is labeled as stratiform.

Figs. 1 and 2 illustrate the application of the BR03 method to our cloud radar and disdrometer data respectively, collected
 130 in Cabauw on May 22nd, 2021, during a 3-hour period of stratiform rain. The BR03 method identified two short convective periods within the event. However, the 35 GHz cloud radar co-polar correlation coefficient reveals a distinct melting layer signature throughout the entire event, which contradicts the classification suggested by BR03.

To avoid issues with an automated procedure for rain type classification, we manually classified each time period based on the available data sources. To be classified as convective, a time period had to meet the following criteria:



- 135
1. Rainfall intensity (by disdrometer) above 10 mm h^{-1} .
 2. No melting layer signature in the cloud radar and MRR.
 3. Convective available potential energy above 1000 J/kg .
 4. Lightning activity in the area around Cabauw.

Table 1 presents an overview of the eight convective events that were identified in this way, together with some basic statistics
140 for R , N_w , D_m and LWC. All eight convective events occurred during late spring and summer and were associated with moist
unstable atmospheric conditions (i.e., thermal convection). The average rainfall intensity for the convective events is between
 15.1 and 123.1 mm h^{-1} and the highest intensity occurred on 19 May 2022 (mean LWC of 6.1 g mm^{-3} and average D_m of
 2.4 mm).

Note that while we are confident that all our convective events were indeed convective, it is likely that some additional cases
145 of convective rainfall were missed because they did not meet all of the requirements mentioned above. However, since the
Netherlands experiences predominantly stratiform rainfall, the inclusion of a few convective cases in the stratiform category is
likely to have minimal impact on the results.

4 Results

4.1 Quality control of DSD data

150 One advantage of having co-located disdrometers is that the DSD measurements can be cross-checked to make sure they are
consistent with each other. Suspicious DSDs are identified in a two-step procedure: First, the D_m values for both disdrome-
ters are calculated from the measured DSD spectra. If the absolute value of the difference in D_m values for two co-located
measurements exceeds 0.5 mm , both DSD spectra are discarded. The 0.5 mm threshold is inspired by the Global Precipitation
Measurement (GPM) mission which states that D_m should be known to within $\pm 0.5 \text{ mm}$ Tokay et al. (2020).

155 This first filter substantially reduces the measurement uncertainty affecting the D_m values. The root mean square difference
(RMSD) on measured D_m values decreases from 0.32 mm to 0.14 mm and the Pearson correlation coefficient increases from
 0.53 to 0.88 . However, the scatter on $\log_{10}(N_w)$ is still high (RMSD of 0.32 and correlation of 0.70). Therefore, a second filter
that uses a relative-error threshold of $\pm 50\%$ on the LWC between Parsivel 1 and 2 is applied. The justification for this second
filter can be found in Eq. (3) which shows the linear relation between N_w and LWC (assuming D_m is known). The use of a
160 relative error threshold means that the DSDs corresponding to low values of LWC (i.e., low rainfall intensities) are filtered
more strictly than the DSDs corresponding to moderate and high values of LWC.

Fig. 3 shows the N_w values in logarithmic scale before and after the two filters on D_m and LWC. We can see that the
combination of these two filters greatly reduces the scatter. The correlation coefficient increases from 0.70 to 0.86 and the
RMSD decreases from 0.32 to 0.16 . The LWC filter also slightly improves the agreement on D_m (correlation coefficient



165 increases from 0.88 to 0.90 and RMSD reduces from 0.14 to 0.12 mm). In total, 19.8% of the DSDs were discarded during the filtering.

4.2 Fitted μ - Λ relationships

First, the overall μ - Λ relationship without any distinction for the rainfall type is presented. For this part, all 1-min pairs of (μ, Λ) values from the two disdrometers were combined into a single dataset and the optimal α and β coefficients of the power-law in
170 Eq. (6) were fitted using non-linear least squares. To assess the effect of the quality control procedure, the analysis was done with and without the D_m -LWC filters. However, to our surprise, the optimal power-law coefficients ($\alpha=1.632$ and $\beta=5.038$) of the $\mu - \Lambda$ relationship with/without filters were almost the same. Similarly, the RMSE values and goodness of fit with/without filters were identical.

The results above are highly encouraging, as they suggest that the suspicious DSDs removed during quality control were
175 mainly affected by random noise rather than systematic errors. Consequently, the filters applied did not significantly impact the overall $\mu - \Lambda$ relationship, except for reducing the measurement uncertainty. Furthermore, this implies that a single disdrometer may suffice to derive representative μ - Λ relationships without requiring co-location.

Next, the stratiform-convective classification procedure as described in Section III C was applied. Note that for this part of the analysis, only the DSD measurements that passed the D_m -LWC filters were used. The obtained μ - Λ relationships for each
180 rainfall type are presented in Fig. 4. We can see that there are two clearly different $\mu - \Lambda$ relationships for the stratiform and convective rain events. Although the DSD data for the convective regime originate from eight distinct events, the (μ, Λ) pairs corresponding to them nicely align with each other along the fitted power law. This is remarkable given that the μ values cover a relatively large range from -1 to 10. The data for the stratiform cases also nicely follow the power-law model, albeit with larger scatter. The μ values corresponding to the stratiform cases also cover a larger range of values from -2 up to 15, with the
185 most probable value being between 2 and 6. Note that μ values exceeding 15 are possible but only the DSDs with $\mu < 15$ were used in this study.

The stratiform relationship shows striking similarity to the results obtained by van Leth et al. (2020) and Gatidis et al. (2020) who also focused on stratiform rain in the Netherlands with low to moderate rainfall intensities. Compared to the convective one, the stratiform relationship predicts higher Λ values for a given μ , which is consistent with lower D_m values.
190 The convective μ - Λ relationship is similar to the ones obtained by Zhang et al. (2001, 2003) in Florida during the summer months in an environment that is prone to convection due to thermal instability and tropical cyclones. It is worth noting that for small μ values between -2 and 4, which correspond to higher rainfall rates, the stratiform and convective relationships are very similar to each other (RMSD = 0.77). For μ values greater than 4, larger deviations between the two relationships can be noted (RMSD = 4.96). The fact that the two relationships diverge for higher μ values can be attributed to the fact that the
195 characteristic drop sizes for a given DSD shape tends to be higher for convective events, which becomes more visible when the DSDs are peaked (i.e., large μ). The fact that the Parsivel struggles to detect small raindrops is unlikely to explain the differences since all suspicious DSDs for which the two co-located disdrometers disagreed with each other were removed prior to analysis.



The significant differences we see between convective and stratiform μ - Λ relationships suggests that choosing a good relationship is key for retrieving physically meaningful and realistic DSDs from polarimetric radar observations, even though the exact consequences of a wrong μ - Λ relation to the DSD retrieval procedure still requires further investigation. Using a single, global μ - Λ relationship regardless of the rainfall type could be problematic, especially for lower rainfall rates and very peaked DSDs.

5 Conclusions

A study was conducted to analyze μ - Λ relationships in convective and stratiform rainfall in the Netherlands. Twenty months of DSD data were collected in Cabauw using two co-located Parsivel² optical disdrometers. A quality control filter on D_m and LWC was applied to eliminate periods during which the two disdrometers showed large disagreement. Subsequently, the data from both sensors were combined, and a new μ - Λ power-law relationship based on the double-moment normalization framework was fitted. According to the results the following conclusions can be drawn.

1. The D_m -LWC filter based on two co-located disdrometers substantially reduces the uncertainty affecting the measured DSDs but does not change the μ - Λ relationship. This means that reliable μ - Λ relationships can be obtained using a single disdrometer.
2. The μ - Λ relationships differ significantly between convective and stratiform precipitation, particularly for higher μ and Λ values, which correspond to more peaked DSDs and lower intensity rainfall (less than 5 mm h^{-1}).
3. The obtained μ - Λ relationships are consistent with other relationships from the literature.
4. The new power-law model looks very similar to previously proposed polynomial models but offers better physical interpretation. For example, Eq. 17 shows how the order of the moments used to fit the DSD data influence the μ - Λ relationship.

While this study gives further insight into μ - Λ relationships and their differences between stratiform and convective rainfall in the Netherlands, it is still necessary to further investigate the impact of having two clearly different relations during DSD retrievals and whether the correct choice of the relationship matters for a given retrieval algorithm and rainfall intensity. Also, more convective-type events should be considered to get a more representative idea of the natural variability of μ - Λ relations within and between events. Currently, a new extended DSD dataset is being prepared, which is expected to provide further insights into these issues.



225 *Author contributions.* CG mainly worked on data processing, visualization of the results and writing (original draft preparation). MS and CU
focused on the supervision of CG with fundamental ideas about the direction of the research, the used methodology and finally the writing
(review and editing).

Competing interests. The authors declare that they have no conflict of interest

230 *Acknowledgements.* This work was supported by the "User Support Programme Space Research 2012-2016", project ALW-GO/15-35 as
well as the Ruisdael Observatory, a scientific research infrastructure co-financed by the Netherlands Organisation for Scientific Research
(NWO), grant number 184.034.015.



References

- Bringi, V. N., Chandrasekar, V., Hubbert, J., Gorgucci, E., Randeu, W. L., and Schoenhuber, M.: Raindrop Size Distribution in Different Climatic Regimes from Disdrometer and Dual-Polarized Radar Analysis, *Journal of the Atmospheric Sciences*, 60, 354–365, [https://doi.org/10.1175/1520-0469\(2003\)060<0354:RSDIDC>2.0.CO;2](https://doi.org/10.1175/1520-0469(2003)060<0354:RSDIDC>2.0.CO;2), 2003.
- Chen, B., Wang, J., and Gong, D.: Raindrop Size Distribution in a Midlatitude Continental Squall Line Measured by Thies Optical Disdrometers over East China, *Journal of Applied Meteorology and Climatology*, 55, 621 – 634, <https://doi.org/10.1175/JAMC-D-15-0127.1>, 2016.
- Chu, Y.-H. and Su, C.-L.: An Investigation of the Slope–Shape Relation for Gamma Raindrop Size Distribution, *Journal of Applied Meteorology and Climatology*, 47, 2531 – 2544, <https://doi.org/https://doi.org/10.1175/2008JAMC1755.1>, 2008.
- Gatidis, C., Schleiss, M., Unal, C., and Russchenberg, H.: A Critical Evaluation of the Adequacy of the Gamma Model for Representing Raindrop Size Distributions, *Journal of Atmospheric and Oceanic Technology*, 37, 1765–1779, <https://doi.org/10.1175/JTECH-D-19-0106.1>, 2020.
- Gatidis, C., Schleiss, M., and Unal, C.: Sensitivity analysis of DSD retrievals from polarimetric radar in stratiform rain based on the μ – Λ relationship, *Atmospheric Measurement Techniques*, 15, 4951–4969, <https://doi.org/10.5194/amt-15-4951-2022>, 2022.
- Lee, G., Zawadzki, I., Szyrmer, W., Sempere-Torres, D., and Uijlenhoet, R.: A general approach to double-moment normalization of drop size distributions, *J. Appl. Meteor.*, 43, 264–281, [https://doi.org/10.1175/1520-0450\(2004\)043<0264:AGATDN>2.0.CO;2](https://doi.org/10.1175/1520-0450(2004)043<0264:AGATDN>2.0.CO;2), 2004.
- Löffler-Mang, M. and Joss, J.: An Optical Disdrometer for Measuring Size and Velocity of Hydrometeors, *Journal of Atmospheric and Oceanic Technology*, 17, 130–139, [https://doi.org/10.1175/1520-0426\(2000\)017<0130:AODFMS>2.0.CO;2](https://doi.org/10.1175/1520-0426(2000)017<0130:AODFMS>2.0.CO;2), 2000.
- Seela, B. K., Janapati, J., Lin, P.-L., Wang, P. K., and Lee, M.-T.: Raindrop Size Distribution Characteristics of Summer and Winter Season Rainfall Over North Taiwan, *Journal of Geophysical Research: Atmospheres*, 123, 11,602–11,624, <https://doi.org/https://doi.org/10.1029/2018JD028307>, 2018.
- Seifert, A.: On the Shape–Slope Relation of Drop Size Distributions in Convective Rain, *Journal of Applied Meteorology*, 44, 1146 – 1151, <https://doi.org/https://doi.org/10.1175/JAM2254.1>, 2005.
- Testud, J., Oury, S., Black, R. A., Amayenc, P., and Dou, X.: The Concept of “Normalized” Distribution to Describe Raindrop Spectra: A Tool for Cloud Physics and Cloud Remote Sensing, *Journal of Applied Meteorology*, 40, 1118–1140, [https://doi.org/10.1175/1520-0450\(2001\)040<1118:TCOND>2.0.CO;2](https://doi.org/10.1175/1520-0450(2001)040<1118:TCOND>2.0.CO;2), 2001.
- Thurai, M., Petersen, W. A., Tokay, A., Schultz, C., and Gatlin, P.: Drop size distribution comparisons between Parsivel and 2-D video disdrometers, *Advances in Geosciences*, 30, 3–9, <https://doi.org/10.5194/adgeo-30-3-2011>, 2011.
- Thurai, M., Williams, C., and Bringi, V.: Examining the correlations between drop size distribution parameters using data from two side-by-side 2D-video disdrometers, *Atmospheric Research*, 144, 95 – 110, <https://doi.org/10.1016/j.atmosres.2014.01.002>, 2014.
- Thurai, M., Bringi, V., Gatlin, P. N., Petersen, W. A., and Wingo, M. T.: Measurements and Modeling of the Full Rain Drop Size Distribution, *Atmosphere*, 10, <https://doi.org/10.3390/atmos10010039>, 2019.
- Tokay, A. and Short, D. A.: Evidence from Tropical Raindrop Spectra of the Origin of Rain from Stratiform versus Convective Clouds, *Journal of Applied Meteorology and Climatology*, 35, 355 – 371, [https://doi.org/10.1175/1520-0450\(1996\)035<0355:EFTRSO>2.0.CO;2](https://doi.org/10.1175/1520-0450(1996)035<0355:EFTRSO>2.0.CO;2), 1996.
- Tokay, A., Wolff, D. B., and Petersen, W. A.: Evaluation of the New Version of the Laser-Optical Disdrometer, OTT Parsivel2, *Journal of Atmospheric and Oceanic Technology*, 31, 1276–1288, <https://doi.org/10.1175/JTECH-D-13-00174.1>, 2014.



- 270 Tokay, A., D'Adderio, L. P., Wolff, D. B., and Petersen, W. A.: Development and Evaluation of the Raindrop Size Distribution Parameters for the NASA Global Precipitation Measurement Mission Ground Validation Program, *Journal of Atmospheric and Oceanic Technology*, 37, 115 – 128, <https://doi.org/https://doi.org/10.1175/JTECH-D-18-0071.1>, 2020.
- Ulbrich, C. W. and Atlas, D.: Microphysics of Raindrop Size Spectra: Tropical Continental and Maritime Storms, *Journal of Applied Meteorology and Climatology*, 46, 1777 – 1791, <https://doi.org/10.1175/2007JAMC1649.1>, 2007.
- van Leth, T. C., Leijnse, H., Overeem, A., and Uijlenhoet, R.: Estimating raindrop size distributions using microwave link measurements: potential and limitations, *Atmospheric Measurement Techniques*, 13, 1797–1815, <https://doi.org/10.5194/amt-13-1797-2020>, 2020.
- 275 Vivekanandan, J., Zhang, G., and Brandes, E.: Polarimetric Radar Estimators Based on a Constrained Gamma Drop Size Distribution Model, *Journal of Applied Meteorology*, 43, 217 – 230, [https://doi.org/https://doi.org/10.1175/1520-0450\(2004\)043<0217:PREBOA>2.0.CO;2](https://doi.org/https://doi.org/10.1175/1520-0450(2004)043<0217:PREBOA>2.0.CO;2), 2004.
- Zhang, G., Vivekanandan, J., and Brandes, E.: A method for estimating rain rate and drop size distribution from polarimetric radar measurements, *IEEE Transactions on Geoscience and Remote Sensing*, 39, 830–841, <https://doi.org/10.1109/36.917906>, 2001.
- 280 Zhang, G., Vivekanandan, J., Brandes, E. A., Meneghini, R., and Kozi, T.: The Shape–Slope Relation in Observed Gamma Rain-drop Size Distributions: Statistical Error or Useful Information?, *Journal of Atmospheric and Oceanic Technology*, 20, 1106–1119, [https://doi.org/10.1175/1520-0426\(2003\)020<1106:TSRIOG>2.0.CO;2](https://doi.org/10.1175/1520-0426(2003)020<1106:TSRIOG>2.0.CO;2), 2003.



Table 1. Overview of the selected convective events. Date, number of 1-minute samples, mean (\bar{x}) and standard deviation (σ) of rain intensity (R), generalized intercept parameter (N_w), mass-weighted mean diameter (D_m) and liquid water content (LWC). Note that the number of samples denotes the total number of 1-min samples available after filtering (both disdrometers combined).

Event	Date	No. of samples	R (\bar{x} / σ) (mm h ⁻¹)	N_w (\bar{x} / σ) (mm ⁻¹ m ⁻³)	D_m (\bar{x} / σ) (mm)	LWC (\bar{x} / σ) (g m ⁻³)
1	17/08/2022	10	32.4 / 13.5	708.3 / 232.9	2.8 / 0.7	1.4 / 0.5
2	30/06/2022	16	15.2 / 4.5	974.7 / 138.1	1.7 / 0.2	0.9 / 0.2
3	24/06/2022	22	66.1 / 33.6	2604.7 / 341.2	2.4 / 0.4	3.5 / 1.6
4	19/05/2022	9	123.1 / 11.1	4460.4 / 597.2	2.4 / 0.2	6.1 / 0.5
5	05/07/2021	19	16.0 / 3.5	1193.0 / 258.3	1.6 / 0.2	1.0 / 0.2
6	04/07/2021	14	15.1 / 4.1	443.8 / 62.7	2.2 / 0.2	0.7 / 0.2
7	03/07/2021 A'	21	18.8 / 8.2	982.9 / 222.2	1.8 / 0.3	1.0 / 0.3
8	03/07/2021 B'	31	20.9 / 5.5	898.1 / 458.5	2.5 / 0.5	1.0 / 0.3
Overall Convective	-	142	30.8 / 29.9	1315.5 / 977.5	2.2 / 0.5	1.6 / 1.5
Overall Stratiform	-	16833	1.8 / 3.9	394.3 / 417.4	1.2 / 0.4	0.2 / 0.4

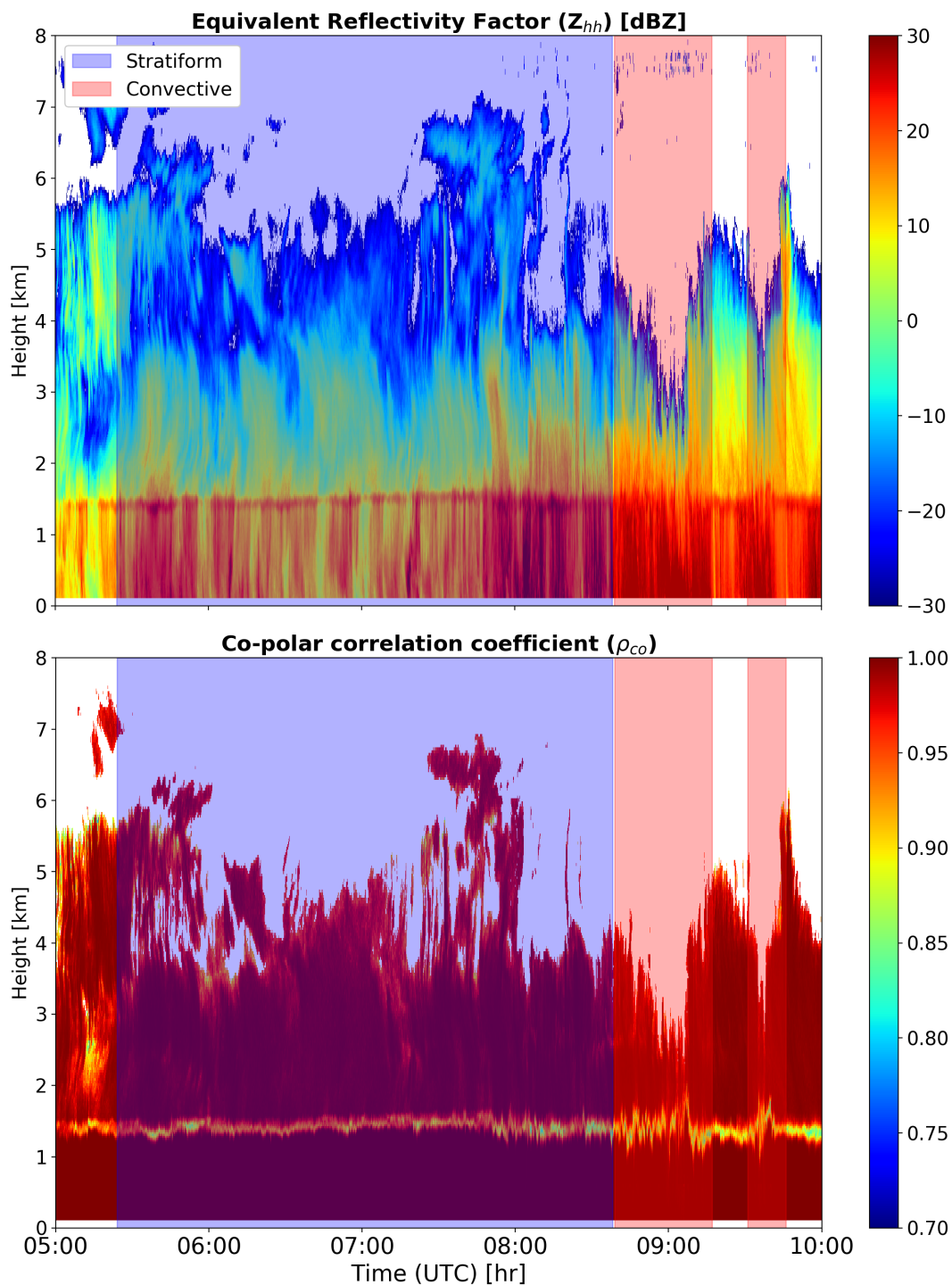


Figure 1. Classification of a stratiform event on May 22nd 2021 based on the BR03 method. Height–time plots (top to bottom) of reflectivity factor (dBZ) and co-polar correlation coefficient from cloud radar.

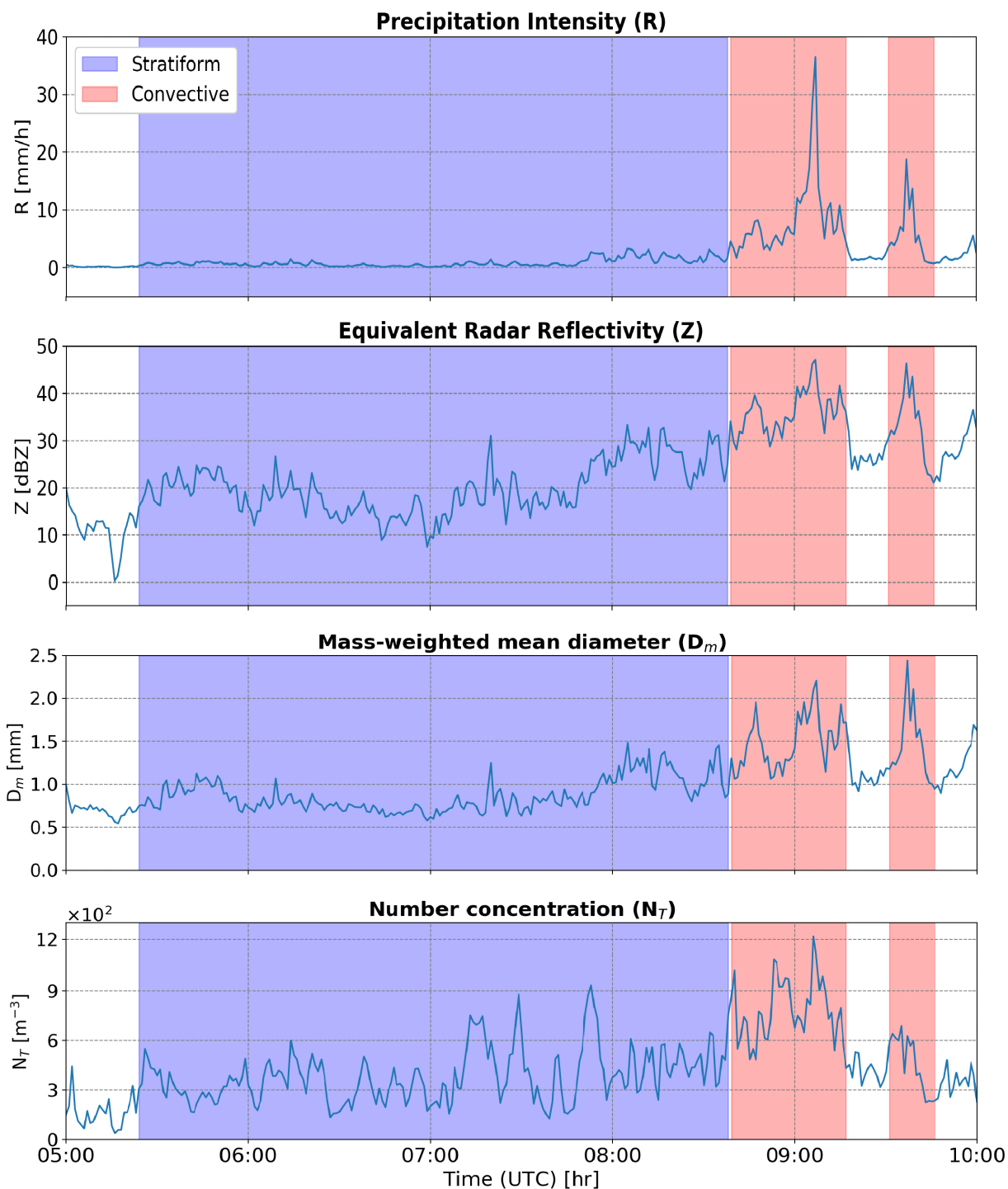


Figure 2. Classification of a stratiform event on May 22nd 2021 based on the BR03 method. Time series (top to bottom) of precipitation intensity (mm h^{-1}), reflectivity factor (dBZ), mass-weighted mean diameter (mm), and number concentration (m^{-3}) from Parsivel disdrometer. Note that after 09:00 there is a peak in rainfall intensity that caused strong attenuation of the radar signal.

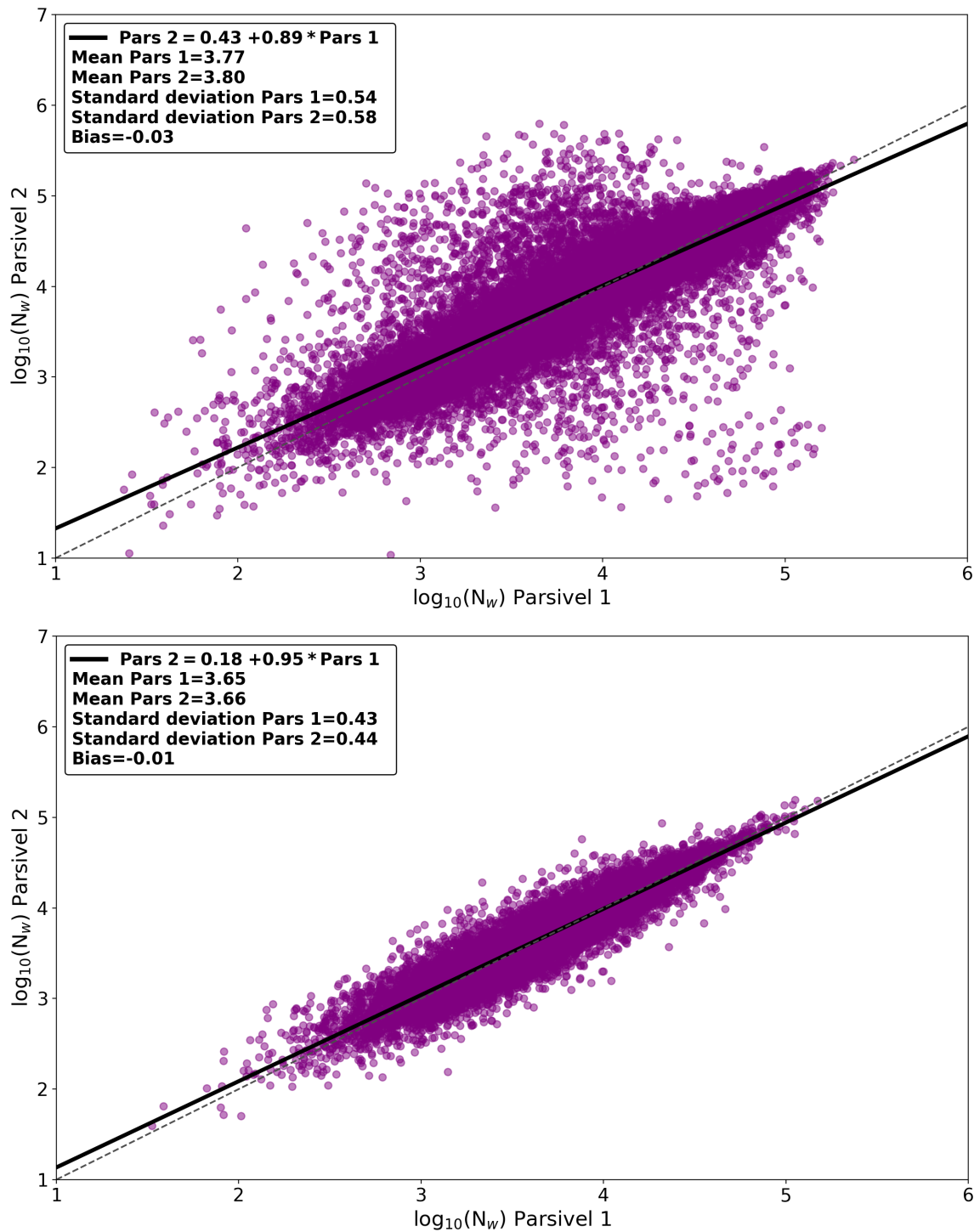


Figure 3. Scatter plots of $\log_{10}N_w$ between Parsivel 1 and Parsivel 2 (top to bottom) before and after D_m and LWC quality control filter.

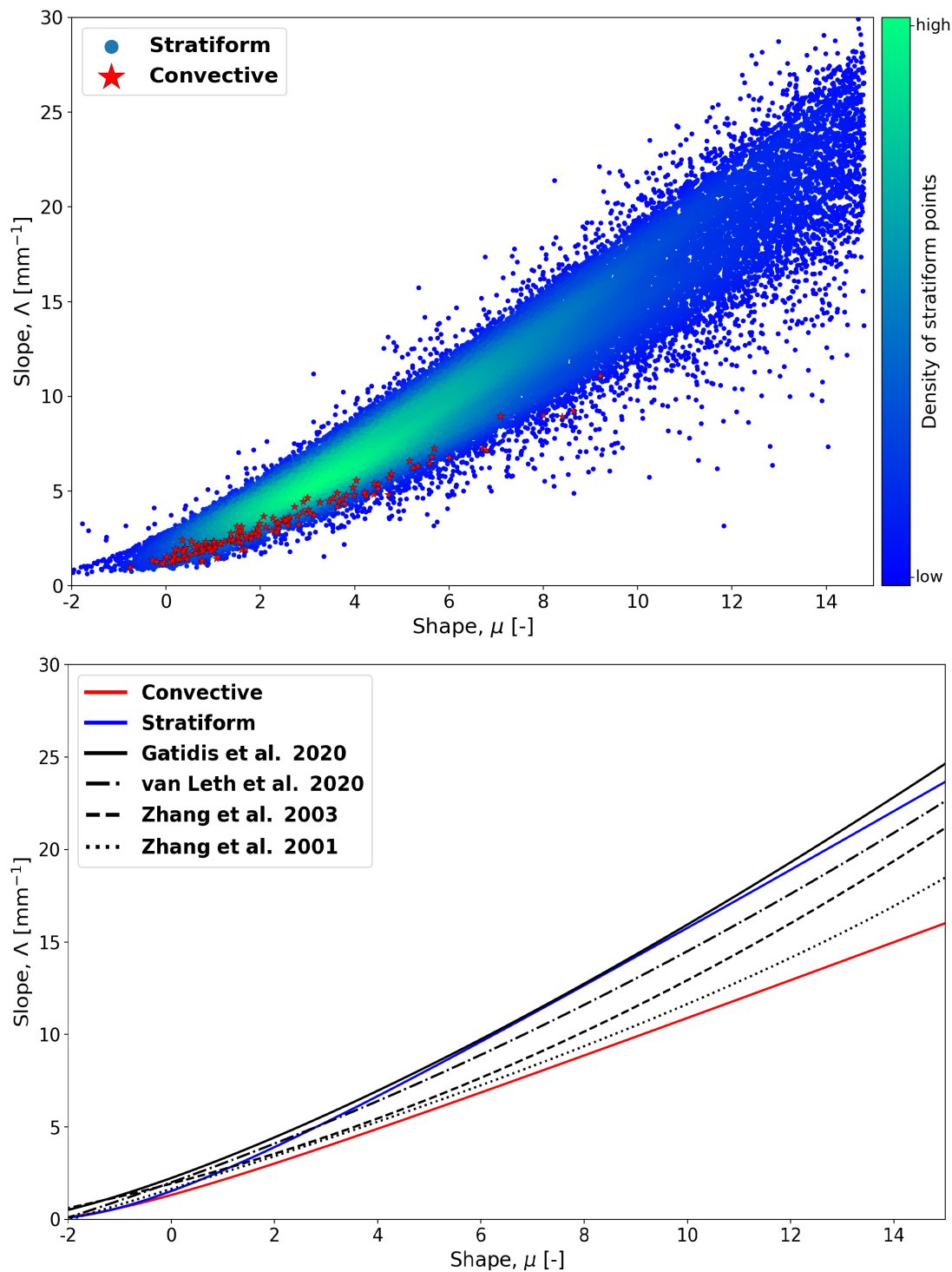


Figure 4. Top panel: $\mu - \Lambda$ pairs for convective rain (stars) and stratiform rain (points). The density of stratiform points increases from blue to green. Bottom panel: $\mu - \Lambda$ relationships for convective and stratiform rain types, together with commonly cited models from the literature.